3620 *Inorg. Chem.* **1993,** *32,* 3620–3627

Edge-Sharing Bioctahedral Dimolybdenum and Dirhenium Compounds with Polydentate Phosphines

F. Albert Cotton,*[†] Bo Hong,[†] Maoyu Shang,[†] and George G. Stanley[‡]

Department of Chemistry and Laboratory for Molecular Structure and Bonding, Texas A&M University, College Station, Texas 77843, and Department of Chemistry, Louisiana State University, Baton Rouge, Louisiana 70803

Received March 9, 1993

The edge-sharing bioctahedral (ESBO) compounds 1,2,7,8-Mo_2Cl_6(*meso*-eLTTP)·C_6H_6 (**2**), (eLTTP = $Et_2PCH_2CH_2P(Ph)CH_2P(Ph)CH_2CH_2PEt_2$), 1,2,5,6-*meso*-$Mo_2Cl_4[Et_2PCH_2CH_2P(Ph)CH_2P(Ph)]_2$·$2C_6H_6$ (**4**), 1,2,7,8-Re_2Cl_6(*meso*-tetraphos-1) (**5**) (tetraphos-1 = $Ph_2PCH_2CH_2P(Ph)CH_2CH_2P(Ph)CH_2CH_2PPh_2$), and 1,2,7,8-$Re_2Cl_6$(*meso*-tetraphos-1)·$(CH_3CH_2)_2O$ (**6**) have been synthesized and structurally determined, and they represent new isomeric forms for the $Mo_2(\mu\text{-}Y)_2X_4P_4$ core. The M–M bond distances are 2.746(1) Å for **1**, 2.8312(3) Å for **4**, and 2.625(1) Å for both **5** and **6**, which all fall within the range established for Mo–Mo and Re–Re bonds in ESBO molecules containing Mo^{III} and Re^{III}. The *meso*-eLTTP ligand adopts a bischelating/single-bridging coordination mode. The diphosphine–phosphido ligand $Et_2PCH_2CH_2P(Ph)CH_2P(Ph)$, which forms by P–C bond cleavage of the original eLTTP ligand with the elimination of one $-CH_2CH_2PEt_2$ unit, adopts a bischelating mode, with the phosphido phosphorus atom occupying the bridging position. The crystal structures of **2** and **4**–**6** are fully described. Crystallographic data for these compounds are as follows: (**2**) space group $P\bar{1}$ with $a = 12.437(2)$ Å, $b = 17.850(3)$ Å, $c = 8.903(1)$ Å, $\alpha = 101.69(1)°$, $\beta = 95.64(1)°$, $\gamma = 91.33(6)$, $V = 1924.3(6)$ Å^3, and $Z = 2$; (**4**) space group $P\bar{1}$ with $a = 11.255(3)$ Å, $b = 12.374(4)$ Å, $c = 10.290(4)$ Å, $\alpha = 98.57(2)°$, $\beta = 96.08(2)°$, $\gamma = 109.21(2)$, $V = 1320(2)$ Å^3, and $Z = 1$; (**5**) space group $P2_1/c$ with $a = 10.234(2)$ Å, $b = 24.908(7)$ Å, $c = 17.889(4)$ Å, $\beta = 93.14(2)°$, $V = 4553(3)$ Å^3, and $Z = 4$; (**6**) space group *Pbca* with $a = 26.519(5)$ Å, $b = 26.335(4)$ Å, $c = 13.976(2)$ Å, $V = 9760(5)$ Å^3, and $Z = 4$.

Introduction

Edge-sharing bioctahedral (ESBO) compounds constitute an important class of complexes containing metal–metal multiple bonds.[1,2] There are two basic synthetic strategies that can be used to produce ESBO compounds. One involves the oxidative addition of an X_2 unit to a quadruply bonded dinuclear species, and the other is the formation of a dinuclear unit from two mononuclear units. Using a recently introduced numbering scheme,[3,4] of which we remind the reader in Figure 1, ESBO complexes with the general formula $M_2(\mu\text{-}Y)_2X_4L_4$, where X and Y are charged ligands and L is a neutral donor ligand, can be designated unambiguously and systematically. A total of nine distinct geometrical isomers, each with a different arrangement of the L ligands, can be obtained: (1) 1,3,5,7 (2) 2,4,6,8 (3) 1,3,6,8 (4) 1,2,7,8 (5) 1,2,5,8 (6) 1,2,6,7 (7) 1,2,5,6 (8) 1,2,5,7 (9) 1,2,6,8

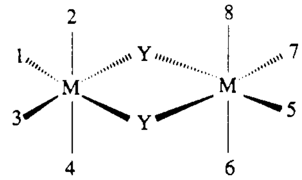

Figure 1. Numbering scheme for the complexes of the $M_2(\mu\text{-}Y)_2X_4L_4$ type.

A recent survey[4] covering about fifty complexes of the type $MM'(\mu\text{-}Y)_2X_4L_4$, where L is limited to neutral phosphine ligands, X, Y are Cl, Br, and I, and M, M′ = Zr, Hf, Nb, Ta, Cr, Mo, W, Re, Ru, and Rh, revealed that there are examples of only six types of geometrical isomers to be found in the literature. The data for the ESBO compounds with M or M′ = Mo, W, and Re are listed in Table I.

For the ESBO complexes with monodentate phosphines, the 1,3,6,8 (3) isomer is the common geometry. However, the metal–metal bond strength may vary, as shown by the change of over 0.9 Å in the metal–metal distance caused by the mere substitution of PEt_3 with PMe_2Ph in the $Mo_2X_6P_4$ class of compounds.[5,6] The electronic properties of the phosphine ligands are thus found to be a decisive factor in the control of the metal–metal bond formation, since these two phosphines have not too dissimilar cone angles (PEt_3, 132°; PMe_2Ph, 122°).[5–7]

For the ESBO complexes with bidentate phosphines, the 1,3,5,7 (1) and 2,4,6,8 (2) isomers are the two common geometries. The metal–metal distances are usually within the ranges established for the appropriate Mo–Mo, W–W, and Re–Re multiple bonds except for that in 1,3,5,7-$Re_2Cl_6(dppe)_2$, which has a nonbonding Re···Re distance of 3.809(1) Å. Few examples of other geometries have been observed. A pair of isostructural complexes, namely, 1,2,5,6-$MoWCl_6(dmpe)_2$ and 1,2,5,6-$W_2Cl_6(dmpe)_2$, are only slightly different in molecular parameters, and they provide a ligand arrangement previously unobserved for $M_2X_6(PP)_2$ type compounds.[3]

The first reported ESBO complex with a tetraphosphine ligand, $MoWCl_6$(*rac*-tetraphos-1), displayed a new type of ligand distribution, 1,2,5,8 (5), for an ESBO complex.[3,4] The arrangement of racemic tetraphos-1 ligand is such that it consists of two chelating diphosphine units and one bridging diphosphine unit, whereby a 2-fold axis orthogonal to the metal–metal axis is the unique element of symmetry in each molecule. The metal–metal bond distance is 2.718(2) Å, essentially an average of the metal–metal distances for 1,3,5,7-$MoWCl_6(dppe)_2$ and 2,4,6,8-$MoWCl_6(dppm)_2$.

[†] Texas A&M University.
[‡] Louisiana State University.

(1) Cotton, F. A.; Walton, R. A. *Multiple Bonds Between Metal Atoms*, 2nd ed.; Oxford University Press: Oxford, U.K., 1993.

(2) Cotton, F. A. *Polyhedron* **1987**, *6*, 667.

(3) Cotton, F. A.; Eglin, J. L.; James, C. A. *Inorg. Chem.* **1993**, *32*, 687.

(4) James, C. A. Dissertation, Texas A&M University, 1992.

(5) Poli, R.; Mui, H. D. *Inorg. Chem.* **1989**, *28*, 3609.

(6) Poli, R.; Mui, H. D. *Inorg. Chem.* **1991**, *30*, 65.

(7) Tolman, C. A. *Chem. Rev.* **1977**, 313.

0020-1669/93/1332-3620$04.00/0

Table I. Data for $MM'(\mu\text{-}Y)_2X_4L_4$ Compounds

complexes	M–M (Å)	isomer type
$Mo_2Cl_6(PEt_3)_4$[5]	3.730(1)	1,3,6,8
$Mo_2Cl_6(PMe_2Ph)_4$[6]	2.8036(8)	1,3,6,8
$W_2Cl_6(PMe_2Ph)_4$[20]	2.6950(3)	1,3,6,8
$Mo_2Cl_6(dmpm)_2$[21]	2.7394(5)	2,4,6,8
$Mo_2Cl_6(dppm)_2$[22]	2.789(1)	2,4,6,8
$Mo_2Cl_4I_2(dppm)_2$[23]	2.827(1)	2,4,6,8
$Mo_2Br_6(dppm)_2$[23]	2.879(2)	2,4,6,8
$Mo_2I_6(dppm)_2$[23]	3.061(1)	2,4,6,8
$W_2Cl_6(dmpm)_2$[21]	2.6663(4)	2,4,6,8
$W_2Cl_6(dppm)_2$[21]	2.691(1)	2,4,6,8
$MoWCl_6(dmpm)_2$[24]	2.682(1)	2,4,6,8
$MoWCl_6(dppm)_2$[24]	2.7230(6)	2,4,6,8
$MoWCl_4(\mu\text{-}Cl)(\mu\text{-}H)(dppm)_2$[25]	2.4932(3)	2,4,6,8
$Re_2Cl_6(dmpm)_2$[21]	2.5807(4)	2,4,6,8
$Re_2Cl_6(dppm)_2$[26]	2.616(1)	2,4,6,8
$Re_2Cl_4(\mu\text{-}SePh)_2(dppm)_2$[28]	2.656(1)	2,4,6,8
$Mo_2Cl_6(dedppe)_2$[27]	2.785(3)	1,3,5,7
$Mo_2Cl_6(dppe)_2$[27]	2.762(1)	1,3,5,7
$W_2Cl_6(dppe)_2$[27]	2.682(1)	1,3,5,7
$Re_2Cl_6(dppe)_2$[26]	3.809(1)	1,3,5,7
$MoWCl_6(dmpe)_2$[2]	2.7028(5)	1,3,5,7
$MoWCl_6(dppe)_2$[24]	2.7123(9)	1,3,5,7
$W_2Cl_6(dmpe)_2$[3]	2.6726(8)	1,2,5,6
$MoWCl_6(dmpe)_2$[3]	2.695(1)	1,2,5,6
$MoWCl_6$(*rac*-tetraphos-1)[3]	2.718(2)	1,2,5,8

None of the remaining four geometrical isomers, 4, 6, 8, and 9, has yet been reported in the literature. We report here the synthesis, structure determination, and spectroscopic study of several new ESBO dimolybdenum and dirhenium compounds with polydentate phosphine ligands, namely, two tetraphosphine ligands, eLTTP[8,9] and tetraphos-1, and one diphosphine–phosphido ligand, $Et_2P(CH_2)_2P(Ph)CH_2P(Ph)$, which is believed to form by P–C bond cleavage in the original eLTTP ligand. These compounds embody two types of geometrical isomeric forms, namely the 1,2,7,8 (4) and 1,2,5,6 (7) types, the first of which has not previously been reported in the literature. Their structural and spectroscopic properties will be discussed.

Results and Discussion

Synthesis and Spectroscopic Study. The reaction of $Mo_2(O_2CCF_3)_4$, 1 equiv of *meso*-eLTTP ligand, and excess Me_3SiCl in THF gives a blue precipitate. The UV–vis spectrum of this product in CH_2Cl_2 shows three distinct bands at 625, 487, and 315 nm, which indicates the existence of a $Mo\overset{4}{-}Mo$ bond with a very small torsional angle according to the previous studies.[10] Chemical analysis confirms the formula of the blue product as Mo_2Cl_4(eLTTP) (**1**). Efforts have been made to obtain the crystal structure of this compound. However, this blue compound is only sparingly soluble in CH_2Cl_2 to give a blue solution, which changes to red after 12 h. The absorption spectrum of this red solution displays no distinct band between 500 and 800 nm and shows a strong peak only at 392 nm. Red crystals were obtained in 10–15% yield from slow diffusion of a hexane/benzene mixture into this red solution, and one of the crystals was used to show that this substance is the ESBO compound 1,2,7,8-Mo_2Cl_6(*meso*-eLTTP)·C_6H_6 (**2**).

The $^{31}P\{^1H\}$ NMR spectrum of a CD_2Cl_2/CH_2Cl_2 (1:3) solution of the blue compound **1** displays two doublets at 45.67 and 55.68 ppm at 298 K, each with J_{P-P} = 4 Hz. Thus this system is diamagnetic. It has been found previously[10a] that two trans P atoms on the same Mo center will give a large ^{31}P–^{31}P coupling constant (ca. 130 Hz) while two cis P atoms on the same Mo center will have a much smaller ^{31}P–^{31}P coupling constant (ca. 10 Hz). On the basis of all the spectroscopic data, the structure shown in Figure 2 can be proposed for complex **1**. It is a quadruply bonded compound with a small average torsional angle. The two central P atoms coordinate to different Mo atoms, and a chelate ring is then formed at each metal atom.

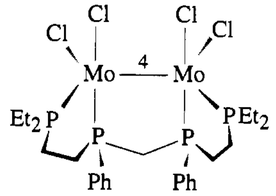

Figure 2. Proposed structure for compound **1**.

The $^{31}P\{^1H\}$ NMR spectrum of compound **2** does not have any distinct band. This may be due, at least in part, to the low solubility of this ESBO compound and perhaps also to partial paramagnetism.

The reaction of $Mo_2Cl_4(PEt_3)_4$ with the 1:1 mixture of the meso and racemic diastereomers of the eLTTP ligand in refluxing toluene for 18 h produces a green solid **3** in 55–65% yield. The absorption spectrum of **3** has three distinct bands in the visible region: 705, 418, and 375 nm. The $^{31}P\{^1H\}$ NMR spectrum of **3** has two doublets at 48.29 and 55.79 ppm, each with J_{P-P} = 3 Hz. Chemical analysis confirms the formula of **3** as Mo_2Cl_4(eLTTP), but the UV–vis and $^{31}P\{^1H\}$ NMR spectra of **3** are different from those of compound **1**. It is thus very likely that compound **3** is another quadruply bonded dimolybdenum compound with the same formula, Mo_2Cl_4(eLTTP), but with a different diastereomeric form and/or a different coordination mode of the ligand, as well as different torsional angles. Furthermore, both the $^{31}P\{^1H\}$ NMR and UV–vis spectra clearly indicate that green solid **3** contains only a single diastereomer of the eLTTP ligand. Since we started with a 1:1 mixture of both *rac*- and *meso*-eLTTP, it is likely that the complex formed by the other diastereomeric form of the eLTTP ligand remained in the brown mother liquor.

Efforts have also been made to obtain the structure of **3**. When this green solid was dissolved in CH_2Cl_2, it gave a brown-green solution. Several brown prismatic and some dark green crystals (ca. 5% yield) appeared after several weeks by slow diffusion of a mixture of benzene/THF (1:1.5) solvents into the CH_2Cl_2 solution. The brown crystals were structurally determined to be the phosphido-bridged ESBO compound **4** with the diphosphine–phosphido ligand $Et_2PCH_2CH_2P(Ph)CH_2PPh$. When comparing the tetraphosphine ligand eLTTP, $Et_2PCH_2CH_2P(Ph)CH_2P(Ph)CH_2CH_2PEt_2$, with this diphosphine–phosphido ligand, it seems evident that the latter is formed by a P–C cleavage reaction leading to the loss of one $-CH_2CH_2PEt_2$ unit.

It has been found previously that when there are metal centers susceptible to oxidative addition, the $R_2PCH_2PR_2$-type ligand cannot necessarily be regarded simply as an inert ligand but must be considered as a potentially oxidizing reagent.[11] This type of ligand may undergo the formal process shown in eq 1. A P–C

$$R_2PCH_2PR_2 \rightarrow R_2P^{\bullet} + R_2PCH_2^{\bullet} \tag{1}$$

bond cleavage product, $[W_2Cl_4(dmpm)_2(\mu\text{-}PMe_2)(\eta^2\text{-}PMe_2CH_2)]^+$, was obtained in the reaction of $W_2Cl_4(PBu_3)_4$ with dmpm in a toluene/hexane mixture.[11a] It was also found previously[12] that when $W(CO)_6$ and the hexaphosphine ligand eHTP, (Et_2P-

---

(8) Lanemen, S. A.; Fronczek, F. R.; Stanley, G. G. *J. Am. Chem. Soc.* **1988**, *110*, 5585.

(9) (a) Lanemen, S. A.; Fronczek, F. R.; Stanley, G. G. *Inorg. Chem.* **1989**, *28*, 1207. (b) Lanemen, S. A.; Fronczek, F. R.; Stanley, G. G. *Inorg. Chem.* **1989**, *28*, 1872.

(10) (a) Cotton, F. A.; Hong, B. *Inorg. Chem.* **1993**, *32*, 2354. (b) Chen, J.-D.; Cotton, F. A.; Hong, B. *Inorg. Chem.* **1993**, *32*, 2343.

(11) (a) Cotton, F. A.; Canich, J. M.; Luck, R. L.; Vidyasager, K. *Organometallics* **1991**, *10*, 352. (b) Doherty, N. M.; Hogarth, G.; Knox, S. A. R.; Macpherson, K. A.; Melchior, F.; Orpen, A. G. *J. Chem. Soc., Chem. Commun.* **1986**, 540.

(12) Saum, S. E.; Fronczek, F. R.; Lanemen, S. A.; Stanley, G. G. *Inorg. Chem.* **1989**, *28*, 1878.

Table II. Crystallographic Data and Data Collection Parameters for **2** and **4–6**

	2	**4**	**5**	**6**
chem formula	$Mo_2Cl_6P_4C_{31}H_{46}$	$Mo_2Cl_4P_6C_{50}H_{64}$	$Re_2Cl_6P_4C_{42}H_{42}$	$Re_2Cl_6P_4O_1C_{46}H_{52}$
fw	947.21	1184.60	1255.82	1329.94
space group	$P\bar{1}$	$P\bar{1}$	$P2_1/c$	*Pbca*
a, Å	12.437(2)	11.255(3)	10.234(2)	26.519(5)
b, Å	17.850(3)	12.374(4)	24.908(7)	26.335(4)
c, Å	8.903(1)	10.290(4)	17.889(4)	13.976(2)
α, deg	101.69(1)	98.57(2)	90	90
β, deg	95.64(1)	96.08(2)	93.14(2)	90
γ, deg	91.33(1)	109.21(2)	90	90
V, Å^3	1924.3(6)	1320(2)	4553(3)	9760(5)
Z	2	1	4	8
T, °C	20 ± 1	20 ± 1	20 ± 1	20 ± 1
λ, Å	1.541 84	1.541 84	1.541 84	0.710 73
ρ_{calcd}, g cm^{-3}	1.634	1.491	1.832	1.810
μ(Mo Kα), cm^{-1}	111.722	78.99	147.829	55.198
data colln instrument	Rigaku AFC5R	Rigaku AFC5R	Rigaku AFC5R	Syntex P3
transm coeff	1.000–0.814	1.000–0.700	1.000–0.237	0.999–0.749
$R(F_o)^a$ $R_w(F_o)^b$	0.0476, 0.0574	0.03466, 0.05440	0.0658, 0.0812	0.06217, 0.07506

[a] $R = \sum||F_o| - |F_c||/\sum|F_o|$. [b] $R_w = [\sum w(|F_o| - |F_c|)^2/\sum w|F_o|^2]^{1/2}$; $w = 1/\sigma^2(|F_o|)$.

$CH_2CH_2)_2PCH_2P(CH_2CH_2PEt_2)_2$, were refluxed in xylene for 5 days, a side product, $W_2(CO)_7(C_{19}H_{43}P_5)$, was obtained, where the eHTP ligand lost one $-CH_2CH_2PEt_2$ arm to form a rather novel pentaphosphine ligand. However, it is not common to have a P–C bond cleavage in the $R_2PCH_2CH_2PR_2$-type of phosphine ligands in a compound with Mo centers. In the present case it appears that the ligand eLTTP undergoes the following type of process

$$[Et_2P(CH_2)_2P(Ph)]_2CH_2 \rightarrow Et_2PCH_2CH_2^{\bullet} + Et_2P(CH_2)_2P(Ph)CH_2P(Ph)^{\bullet} \quad (2)$$

However, this P–C cleavage process is only a side reaction since the major product is shown by spectroscopic studies to be the quadruply bonded compound Mo_2Cl_4(eLTTP). It is also not clear whether the process of eq 2 takes place before or after the formation of compound **3**. Unfortunately, the green crystals of **3** were persistently twinned and no proper model was found to solve the structure.

When $(NBu^n_4)_2Re_2Cl_8$ and tetraphos-1 ligand react in refluxing CH_2Cl_2, a red precipitate is obtained in low yield (5–15%) and a brown-yellow solid (**7**) is obtained from the mother liquor in 65–75% yield after evaporation of the solvent. The red solid has very low solubilities in most organic solvents and is only slightly soluble in MeCN and CH_2Cl_2. Thin plate and needle crystals were obtained by slow diffusion of a hexane/diethyl ether (1:2) mixture into the MeCN solution of this red product, and it has been shown that they both contain the meso diastereomer of the tetraphos-1 ligand. The two substances are Re_2Cl_6(*meso*-tetraphos-1) (**5**) and Re_2Cl_6(*meso*-tetraphos-1)$\cdot(CH_3CH_2)_2O$ (**6**). For the brown-yellow product **7**, though it is quite soluble in CH_2Cl_2, no crystal was obtained using the slow diffusion method in different solvent systems, such as THF/CH_2Cl_2, benzene/CH_2Cl_2, MeCN/CH_2Cl_2, etc. The absorption spectrum of **7** displays two distinct bands at 682 and 382 nm in the visible region. The $^{31}P\{^1H\}$ NMR spectrum of **7** shows four multiplets at δ 53.6, 51.1, 41.5, and 32.1 ppm at 273 K. Chemical analysis of this product indicates that its formula is close to Re_2Cl_4(tetraphos-1). However, at this stage much further work is required on this material.

Structure and Bonding

Pertinent crystallographic information on the four structures that were obtained is given in Table II. Tables III–VI list the positional and thermal parameters for complex **2** and **4–6**, respectively.

Table III. Positional and Thermal Parameters for Non-Hydrogen Atoms of 1,2,7,8-Mo_2Cl_6(*meso*-eLTTP)$\cdot C_6H_6$ (**2**)

atom	*x*	*y*	*z*	B_{eq} (Å^2)^a
Mo(1)	0.80989(7)	0.69230(6)	0.1953(1)	3.08(2)
Mo(2)	0.67382(7)	0.81204(5)	0.2116(1)	3.00(2)
Cl(1)	0.6201(2)	0.6824(2)	0.2152(3)	3.32(6)
Cl(2)	0.8612(2)	0.8194(2)	0.1630(3)	4.36(7)
Cl(3)	1.0016(3)	0.6711(2)	0.2060(4)	5.09(8)
Cl(4)	0.7832(3)	0.6373(2)	−0.0770(3)	5.15(8)
Cl(5)	0.6833(3)	0.9496(2)	0.2339(4)	5.14(8)
Cl(6)	0.6069(3)	0.7917(2)	−0.0567(3)	4.69(7)
P(1)	0.8021(3)	0.5549(2)	0.2323(4)	4.39(8)
P(2)	0.8395(3)	0.7121(2)	0.4852(3)	3.84(7)
P(3)	0.6919(2)	0.8400(2)	0.5040(3)	3.32(6)
P(4)	0.4768(3)	0.8306(2)	0.2622(4)	4.24(8)
C(1)	0.675(1)	0.4976(9)	0.197(2)	9.0(5)
C(2)	0.640(2)	0.472(1)	0.030(3)	14.4(7)
C(3)	0.896(1)	0.4908(9)	0.130(2)	6.9(4)
C(4)	0.904(1)	0.4109(8)	0.174(2)	8.0(5)
C(5)	0.836(3)	0.5566(9)	0.432(2)	16(1)
C(6)	0.844(2)	0.6159(8)	0.536(1)	7.9(5)
C(7)	0.957(1)	0.7676(7)	0.598(1)	4.3(3)
C(8)	0.973(1)	0.7656(8)	0.756(1)	5.4(3)
C(9)	1.062(1)	0.806(1)	0.849(2)	7.4(5)
C(10)	1.126(1)	0.8498(8)	0.781(2)	7.0(4)
C(11)	1.114(1)	0.8531(8)	0.622(2)	7.5(5)
C(12)	1.025(1)	0.8096(7)	0.530(2)	5.3(3)
C(13)	0.724(1)	0.7515(6)	0.577(1)	4.0(3)
C(14)	0.7825(8)	0.9130(6)	0.629(1)	3.3(2)
C(15)	0.7842(9)	0.9223(7)	0.786(1)	3.8(3)
C(16)	0.853(1)	0.9778(8)	0.885(1)	4.9(3)
C(17)	0.918(1)	1.0246(8)	0.822(2)	5.2(3)
C(18)	0.918(1)	1.0171(7)	0.664(1)	4.7(3)
C(19)	0.848(1)	0.9607(7)	0.565(1)	4.1(3)
C(20)	0.5583(9)	0.8665(8)	0.570(1)	4.9(3)
C(21)	0.464(1)	0.8241(9)	0.462(2)	6.5(4)
C(22)	0.377(1)	0.7539(8)	0.159(2)	6.1(4)
C(23)	0.258(1)	0.7701(9)	0.187(2)	6.9(4)
C(24)	0.417(1)	0.9187(8)	0.234(2)	7.2(4)
C(25)	0.405(1)	0.925(1)	0.066(2)	9.2(5)
C(26)	0.750(2)	0.342(1)	0.488(2)	12.6(6)
C(27)	0.716(2)	0.398(1)	0.600(2)	12.4(8)
C(28)	0.612(2)	0.425(1)	0.588(2)	10.9(6)
C(29)	0.540(1)	0.395(1)	0.461(2)	9.4(5)
C(30)	0.569(2)	0.3394(9)	0.346(2)	9.5(5)
C(31)	0.675(2)	0.3135(9)	0.363(2)	12.1(5)

[a] B values for anisotropically refined atoms are given in the form of the equivalent isotropic displacement parameter defined as $^1/_3[a^2a^{*2}B_{11} + b^2b^{*2}B_{22} + c^2c^{*2}B_{33} + 2ab(\cos\gamma)a^*b^*B_{12} + 2ac(\cos\beta)a^*c^*B_{13} + 2bc(\cos\alpha)b^*c^*B_{23}]$.

Compound 2. Compound **2** crystallizes in the space group $P\bar{1}$ with two molecules per unit cell. As shown in Figure 3, the structure of this ESBO compound shows it to be a 1,2,7,8 (4) type isomer with the two central P atoms coordinating to different Mo centers in axial positions and the two terminal P atoms in equatorial positions. Thus the coordination mode of the *meso*-

Table IV. Positional and Thermal Parameters for Non-Hydrogen Atoms of *meso*-$Mo_2Cl_4[Et_2P(CH_2)_2P(Ph)CH_2P(Ph)]_2 \cdot 2C_6H_6$ (4)

atom	*x*	*y*	*z*	B_{eq} (Å^2)[a]
Mo(1)	0.62251(2)	0.06120(2)	0.47341(2)	2.243(5)
Cl(1)	0.61844(8)	0.25096(7)	0.44444(90	3.44(2)
Cl(2)	0.73662(8)	0.02657(8)	0.28797(9)	3.68(2)
P(1)	0.56676(8)	0.03456(7)	0.68762(8)	2.57(2)
P(2)	0.70272(8)	–0.07994(7)	0.57116(9)	2.75(2)
P(3)	0.84725(9)	0.19337(8)	0.5939(1)	3.16(2)
C(1)	0.6474(3)	–0.0668(3)	0.7316(4)	3.13(8)
C(2)	0.8768(3)	–0.0168(3)	0.6162(4)	3.81(9)
C(3)	0.9233(4)	0.1125(3)	0.6883(5)	4.4(1)
C(4)	0.9648(4)	0.2496(4)	0.4878(4)	4.2(1)
C(5)	0.9389(5)	0.3351(4)	0.4082(5)	5.6(1)
C(6)	0.8633(4)	0.3225(3)	0.7163(4)	4.2(1)
C(7)	0.9996(5)	0.3994(4)	0.7817(5)	5.7(1)
C(8)	0.6845(3)	–0.2301(3)	0.5042(4)	3.15(8)
C(9)	0.6916(4)	–0.2596(3)	0.3720(4)	3.78(9)
C(10)	0.6861(4)	–0.3727(3)	0.3200(4)	4.6(1)
C(11)	0.6742(4)	–0.4531(3)	0.3993(5)	4.9(1)
C(12)	0.6669(5)	–0.4229(3)	0.5320(5)	5.0(1)
C(13)	0.6715(4)	–0.3122(3)	0.5836(4)	4.4(1)
C(14)	0.5872(3)	0.1409(3)	0.8359(3)	2.96(7)
C(15)	0.6199(4)	0.1245(4)	0.9623(4)	4.2(1)
C(16)	0.6333(5)	0.2093(5)	1.0726(4)	6.0(1)
C(17)	0.6134(6)	0.3094(5)	1.0564(5)	7.2(1)
C(18)	0.5792(5)	0.3273(4)	0.9313(5)	6.1(1)
C(19)	0.5673(4)	0.2437(3)	0.8207(4)	4.00(9)
C(20)	0.2432(8)	0.2157(7)	–0.0001(7)	10.5(2)
C(21)	0.2776(8)	0.3312(6)	0.0484(7)	11.0(2)
C(22)	0.191(1)	0.3754(8)	0.1015(9)	12.8(3)
C(23)	0.063(1)	0.2890(9)	0.0960(8)	15.3(4)
C(24)	0.0373(9)	0.186(1)	0.068(1)	14.9(4)
C(25)	0.130(1)	0.138(1)	0.005(1)	15.4(4)

[a] *B* values for anisotropically refined atoms are given in the form of the equivalent isotropic displacement parameter defined as $^1/_3[a^2a^{*2}B_{11} + b^2b^{*2}B_{22} + c^2c^{*2}B_{33} + 2ab(\cos\gamma)a^*b^*B_{12} + 2ac(\cos\beta)a^*c^*B_{13} + 2bc(\cos\alpha)b^*c^*B_{23}]$.

eLTTP ligand is bischelating/single-bridging. Compared with the compound 1,2,5,8-$MoWCl_6$(*rac*-tetraphos-1)[3] and all the other ESBO complexes with mono- or bidentate phosphines (Table I), compound **2** is significant since it is the first example of the geometrical type 1,2,7,8 (4). It is very likely that its meso nature (*R,S* or *S,R*) forces the eLTTP ligand in **2** to adopt this unprecedented geometry, while the racemic nature (*R,R* or *S,S*) of the tetraphos-1 ligand in compound $MoWCl_6$(*rac*-tetraphos-1) drives it to adopt a different geometry. However, since we have not been able to obtain the structure of the analogues Mo_2Cl_6(*meso*-tetraphos-1) and $MoWCl_6$(*rac*-eLTTP), we cannot at this point rule out the possibility that the changes of the connecting chain lengths between the two central phosphorus donor atoms and/or the changes in the terminal groups may also play a role in determining which set of sites are occupied by the four phosphorus atoms.

The Mo–Mo bond distance is 2.746(1) Å, which falls within the metal–metal bond distance range established for Mo–Mo bonds in $Mo_2Cl_6P_4$ compounds. The average Mo–P and Mo–Cl distances are 2.538(3) and 2.411(3) Å, respectively. Selected bond distances and angles are listed in Table VII.

Compound 4. Crystals of **4** conform to the space group $P\bar{1}$, and there is one molecule, which resides on the inversion center, per unit cell. The Mo–Mo bond distance is 2.8312(3) Å. Each diphosphine–phosphido ligand, $Et_2PCH_2CH_2P(Ph)CH_2P(Ph)$, in the molecule is tridentate to one Mo center with the phosphido P atom then forming a Mo–P–Mo bridge (Figure 4). This molecule is the meso diastereomer since each diphosphine–phosphido ligand has but one chiral P center and the two ligands in each molecule of compound **4** are related by an inversion center. Three features of particular interest about the chemistry and structure of this compound are as follows: First, the scission of a tetraphosphine ligand on the Mo centers to form a diphosphine–phosphido ligand; second, the bischelating coordination mode of the diphosphine–phosphido ligand and the bridging terminal –P(Ph) group of this ligand, which gives rise to the fused four-membered and five-membered rings; third, the 1,2,5,6-type geometry (ignore the bridging –P(Ph)), which has previously been reported only in 1,2,5,6-$MoWCl_6(dmpe)_2$ and 1,2,5,6-$W_2Cl_6(dmpe)_2$ for complexes of $M_2X_6P_4$ type. Selected bond distances and angles are listed in Table VIII. The structure is twisted from the ideal edge-sharing bioctahedral geometry due to the bischelating mode of the diphosphine–phosphido ligands.

Table V. Positional and Thermal Parameters for Non-Hydrogen Atoms of 1,2,7,8-Re_2Cl_6(*meso*-tetraphos-1) (5)

atom	*x*	*y*	*z*	B_{eq} (Å^2)[a]
Re(1)	0.04178(7)	0.20613(4)	0.49604(5)	3.22(2)
Re(2)	–0.15961(7)	0.20887(4)	0.39870(5)	3.31(2)
Cl(2)	–0.1554(4)	0.2562(2)	0.5158(3)	4.0(1)
Cl(3)	–0.0358(4)	0.1397(2)	0.5811(3)	4.0(1)
Cl(4)	0.1263(4)	0.2523(2)	0.6053(3)	4.5(1)
Cl(5)	–0.2829(4)	0.1391(2)	0.4548(3)	4.5(1)
Cl(6)	–0.3685(4)	0.2506(3)	0.3738(3)	4.9(1)
P(1)	0.2532(4)	0.1560(2)	0.5081(3)	4.1(1)
P(2)	0.1751(4)	0.2705(2)	0.4377(3)	3.9(1)
P(3)	–0.1061(5)	0.2818(2)	0.3160(3)	4.2(1)
P(4)	–0.2144(5)	0.1632(3)	0.2786(3)	4.3(1)
C(1)	0.369(2)	0.192(1)	0.450(2)	6.9(7)
C(2)	0.349(2)	0.253(1)	0.466(1)	4.7(5)
C(3)	0.175(2)	0.265(1)	0.335(1)	5.1(5)
C(4)	0.067(2)	0.301(1)	0.296(1)	5.2(6)
C(5)	–0.175(2)	0.264(1)	0.220(1)	5.1(5)
C(6)	–0.139(2)	0.203(1)	0.206(1)	5.7(6)
C(7)	0.334(2)	0.152(1)	0.604(1)	5.3(6)
C(8)	0.284(2)	0.126(2)	0.650(2)	10(1)
C(9)	0.349(3)	0.115(2)	0.724(2)	12(1)
C(10)	0.453(3)	0.146(2)	0.740(2)	14(1)
C(11)	0.524(4)	0.148(2)	0.677(3)	21(2)
C(12)	0.441(3)	0.176(2)	0.622(2)	20(1)
C(13)	0.262(2)	0.0822(9)	0.475(1)	3.5(4)
C(14)	0.161(2)	0.051(1)	0.479(1)	5.1(5)
C(15)	0.176(3)	–0.001(1)	0.460(2)	7.4(8)
C(16)	0.292(2)	–0.019(1)	0.429(1)	5.4(6)
C(17)	0.391(2)	0.014(1)	0.424(2)	7.2(7)
C(18)	0.383(2)	0.069(1)	0.450(2)	6.4(7)
C(19)	0.169(2)	0.3423(9)	0.458(1)	4.2(5)
C(20)	0.073(2)	0.363(1)	0.499(2)	7.4(7)
C(21)	0.069(3)	0.419(1)	0.512(1)	7.2(7)
C(22)	0.173(3)	0.450(1)	0.484(2)	10(1)
C(23)	0.264(3)	0.431(1)	0.439(3)	13(1)
C(24)	0.269(2)	0.374(1)	0.432(2)	7.1(7)
C(25)	–0.177(2)	0.3485(9)	0.329(1)	5.0(5)
C(26)	–0.226(2)	0.366(1)	0.396(2)	7.1(7)
C(27)	–0.279(3)	0.417(1)	0.399(2)	7.6(8)
C(28)	–0.286(3)	0.451(1)	0.341(2)	7.0(7)
C(29)	–0.231(3)	0.434(1)	0.277(2)	8.7(8)
C(30)	–0.178(3)	0.384(1)	0.267(2)	7.7(8)
C(31)	–0.389(2)	0.156(1)	0.250(2)	7.0(7)
C(32)	–0.442(4)	0.185(2)	0.197(3)	25(2)
C(33)	–0.555(3)	0.163(2)	0.154(3)	35(1)
C(34)	–0.641(3)	0.139(2)	0.200(3)	16(1)
C(35)	–0.600(2)	0.115(2)	0.261(2)	10(1)
C(36)	–0.465(2)	0.122(2)	0.284(2)	9.3(9)
C(37)	–0.151(2)	0.0954(9)	0.266(1)	4.6(5)
C(38)	–0.163(3)	0.056(1)	0.322(2)	8.4(8)
C(39)	–0.128(3)	0.005(1)	0.310(2)	10(1)
C(40)	–0.071(4)	–0.011(1)	0.246(2)	10(1)
C(41)	–0.052(4)	0.026(2)	0.196(2)	12(1)
C(42)	–0.093(3)	0.082(1)	0.204(2)	10(1)

[a] *B* values for anisotropically refined atoms are given in the form of the equivalent isotropic displacement parameter defined as $^1/_3[a^2a^{*2}B_{11} + b^2b^{*2}B_{22} + c^2c^{*2}B_{33} + 2ab(\cos\gamma)a^*b^*B_{12} + 2ac(\cos\beta)a^*c^*B_{13} + 2bc(\cos\alpha)b^*c^*B_{23}]$.

Compounds 5 and 6. Crystals of compound **5** conform to the space group $P2_1/c$, and compound **6** crystallizes in the orthorhombic space group *Pbca*. Selected bond distances and angles are listed in Tables IX and X, respectively. The differences in the unit cell arrangements of these two compounds are best observed by inspection of the unit cell packing diagrams, which

Table VI. Positional and Thermal Parameters for Non-Hydrogen Atoms of 1,2,7,8-Re_2Cl_6(*meso*-tetraphos-1)·$(CH_3CH_2)_2O$ (6)

atom	*x*	*y*	*z*	B_{eq} (Å^2)[a]
Re(1)	0.20784(5)	0.16735(4)	0.04490(7)	2.00(2)
Re(2)	0.21305(5)	0.06791(4)	0.03653(7)	1.87(2)
Cl(1)	0.1556(3)	0.1176(3)	0.0531(4)	2.5(1)
Cl(2)	0.2585(3)	0.1178(3)	0.1534(4)	2.6(1)
Cl(3)	0.2487(3)	0.2386(3)	0.1193(5)	3.2(2)
Cl(4)	0.1454(3)	0.1725(3)	0.1687(5)	2.7(2)
Cl(5)	0.2587(3)	−0.0025(3)	0.1046(5)	2.6(2)
Cl(6)	0.1512(3)	0.0490(3)	0.1579(5)	3.0(2)
P(1)	0.1594(3)	0.2358(3)	−0.0375(6)	2.8(2)
P(2)	0.2665(4)	0.1854(3)	−0.0792(5)	2.7(2)
P(3)	0.2760(4)	0.0549(3)	−0.0842(5)	2.7(2)
P(4)	0.1696(3)	0.0004(3)	−0.0541(6)	2.4(2)
C(1)	0.195(1)	0.252(1)	−0.149(2)	5.0(9)
C(2)	0.250(1)	0.252(1)	−0.126(2)	2.5(6)*
C(3)	0.254(2)	0.149(1)	−0.190(2)	4.4(9)
C(4)	0.275(2)	0.092(1)	−0.195(2)	6(1)
C(5)	0.266(1)	−0.010(1)	−0.135(2)	2.4(6)*
C(6)	0.210(1)	−0.0137(9)	−0.159(2)	1.8(5)*
C(7)	0.148(2)	0.297(2)	0.024(3)	5.6(9)*
C(8)	0.120(2)	0.295(2)	0.110(3)	7(1)*
C(9)	0.112(2)	0.344(1)	0.157(3)	8(1)
C(10)	0.136(2)	0.389(1)	0.122(3)	9(2)
C(11)	0.163(2)	0.385(2)	0.044(4)	12(2)*
C(12)	0.171(2)	0.339(1)	−0.009(4)	9(1)
C(13)	0.093(1)	0.224(1)	−0.079(2)	2.1(6)*
C(14)	0.081(1)	0.248(1)	−0.161(2)	4.1(8)
C(15)	0.029(2)	0.241(2)	−0.186(3)	7(1)
C(16)	−0.003(1)	0.213(1)	−0.140(2)	4.1(8)
C(17)	0.013(1)	0.188(1)	−0.056(3)	4.3(8)
C(18)	0.061(1)	0.193(1)	−0.025(2)	2.7(6)*
C(19)	0.336(1)	0.189(1)	−0.062(2)	2.5(6)*
C(20)	0.356(1)	0.187(1)	0.025(2)	3.0(6)*
C(21)	0.410(2)	0.194(2)	0.038(3)	7(1)*
C(22)	0.440(2)	0.198(2)	−0.043(3)	8(1)
C(23)	0.413(2)	0.199(3)	−0.131(4)	12(2)
C(24)	0.366(2)	0.193(2)	−0.147(4)	10(2)*
C(25)	0.344(1)	0.051(1)	−0.057(2)	3.9(8)
C(26)	0.376(2)	0.029(2)	−0.123(3)	6(1)
C(27)	0.428(1)	0.025(2)	−0.106(3)	6(1)
C(28)	0.445(2)	0.046(2)	−0.016(3)	7(1)
C(29)	0.413(1)	0.064(1)	0.051(3)	4.8(9)
C(30)	0.362(1)	0.067(1)	0.035(3)	5.1(9)
C(31)	0.161(1)	−0.062(1)	0.004(2)	2.0(6)*
C(32)	0.198(2)	−0.098(1)	0.000(2)	4.6(9)
C(33)	0.186(2)	−0.147(1)	0.044(2)	5.4(9)
C(34)	0.145(1)	−0.155(1)	0.100(2)	3.8(8)
C(35)	0.109(1)	−0.117(1)	0.111(3)	4.7(8)*
C(36)	0.116(1)	−0.068(1)	0.067(2)	3.6(8)
C(37)	0.108(1)	0.013(1)	−0.101(2)	4.3(9)
C(38)	0.096(1)	0.003(1)	−0.201(2)	3.5(8)
C(39)	0.049(2)	0.016(2)	−0.228(2)	6(1)
C(40)	0.010(2)	0.037(2)	−0.176(3)	6(1)
C(41)	0.022(2)	0.045(1)	−0.077(3)	4.5(9)
C(42)	0.072(1)	0.036(1)	−0.043(2)	3.3(7)
C(43)	0.543(2)	0.109(2)	0.179(4)	9(2)
C(44)	0.514(2)	0.120(2)	0.275(4)	10(2)
O(1)	0.466(1)	0.134(1)	0.253(2)	9.5(9)
C(45)	0.430(2)	0.147(2)	0.330(3)	11(2)
C(46)	0.381(2)	0.158(2)	0.295(3)	9(2)

[a] *B* values for anisotropically refined atoms are given in the form of the equivalent isotropic displacement parameter defined as $^1/_3[a^2a^{*2}B_{11} + b^1b^{*2}B_{22} + c^1c^{*2}B_{33} + 2ab(\cos\gamma)a^*b^*B_{12} + 2ac(\cos\beta)a^*c^*B_{13} + 2bc(\cos\alpha)b^*c^*B_{23}]$. Starred *B* values are for atoms that were refined isotropically.

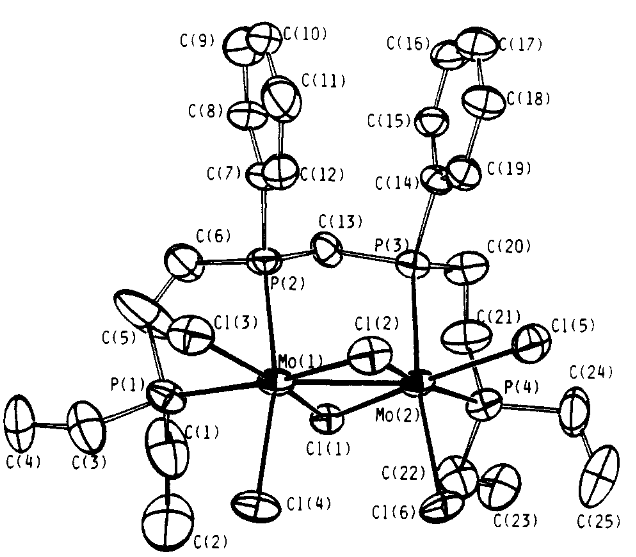

Figure 3. ORTEP drawing of 1,2,7,8-Mo_2Cl_6(*meso*-eLTTP)·C_6H_6 (**2**). Thermal ellipsoids are drawn at the 50% probability level.

Table VII. Selected Bond Lengths (Å) and Angles (deg) for 1,2,7,8-Mo_2Cl_6(*meso*-eLTTP)·C_6H_6 (2)[a]

Distances			
Mo(1)–Mo(2)	2.746(1)	Mo(2)–Cl(5)	2.423(3)
Mo(1)–Cl(1)	2.389(3)	Mo(2)–Cl(6)	2.403(3)
Mo(1)–Cl(2)	2.424(3)	Mo(1)–P(1)	2.541(4)
Mo(1)–Cl(3)	2.417(3)	Mo(1)–P(2)	2.522(3)
Mo(1)–Cl(4)	2.412(3)	Mo(2)–P(3)	2.536(3)
Mo(2)–Cl(1)	2.403(3)	Mo(2)–P(4)	2.551(3)
Mo(2)–Cl(2)	2.417(3)		
Angles			
Mo(2)–Mo(1)–Cl(1)	55.27(7)	Mo(1)–Mo(2)–Cl(6)	98.45(9)
Mo(2)–Mo(1)–Cl(2)	55.32(8)	Mo(1)–Mo(2)–P(3)	92.99(8)
Mo(2)–Mo(1)–Cl(3)	138.9(1)	Mo(1)–Mo(2)–P(4)	135.01(9)
Mo(2)–Mo(1)–Cl(4)	100.8(1)	Cl(1)–Mo(2)–Cl(2)	110.1(1)
Mo(2)–Mo(1)–P(1)	137.39(9)	Cl(1)–Mo(2)–Cl(5)	165.1(1)
Mo(2)–Mo(1)–P(2)	91.63(8)	Cl(1)–Mo(2)–Cl(6)	90.0(1)
Cl(1)–Mo(1)–Cl(2)	110.3(1)	Cl(1)–Mo(2)–P(3)	88.3(1)
Cl(1)–Mo(2)–Cl(3)	164.1(1)	Cl(1)–Mo(2)–P(4)	80.5(1)
Cl(1)–Mo(2)–Cl(4)	91.4(1)	Cl(2)–Mo(2)–Cl(5)	84.6(1)
Cl(1)–Mo(1)–P(1)	82.7(1)	Cl(2)–Mo(2)–Cl(6)	93.8(1)
Cl(1)–Mo(1)–P(2)	87.9(1)	Cl(2)–Mo(2)–P(3)	101.1(1)
Cl(2)–Mo(1)–Cl(3)	85.0(1)	Cl(2)–Mo(2)–P(4)	169.4(1)
Cl(2)–Mo(1)–Cl(4)	95.0(1)	Cl(5)–Mo(2)–Cl(6)	91.7(1)
Cl(2)–Mo(1)–P91)	166.9(1)	Cl(5)–Mo(2)–P(3)	86.2(1)
Cl(2)–Mo(1)–P(2)	99.8(1)	Cl(5)–Mo(2)–P(4)	84.9(1)
Cl(3)–Mo(1)–Cl(4)	91.9(1)	Cl(6)–Mo(2)–P(3)	164.7(1)
Cl(3)–Mo(1)–P(1)	82.0(1)	Cl(6)–Mo(2)–P(4)	85.5(1)
Cl(3)–Mo(1)–P(2)	84.8(1)	P(3)–Mo(2)–P(4)	79.2(1)
Cl(4)–Mo(1)–P(1)	85.6(1)	Mo(1)–Cl(1)–Mo(2)	69.93(8)
Cl(4)–Mo(1)–P(2)	164.4(1)	Mo(1)–Cl(2)–Mo(2)	69.11(9)
P(1)–Mo(1)–P(2)	78.9(1)	Mo(1)–Mo(2)–Cl(1)	54.81(7)
Mo(1)–Mo(2)–Cl(2)	55.57(8)	Mo(1)–Mo(2)–Cl(5)	139.3(1)

[a] Numbers in parentheses are estimated standard deviations in the least significant digit.

are represented in the form of unit cell plots in Figure 5. The unit cell geometry is clearly changed due to the presence of the solvent molecule in **6**.

The ORTEP drawings for compounds **5** and **6** are presented in Figures 6 and 7, respectively. In both cases the molecules reside on general positions and the positions of the heavier atoms were readily apparent from the Patterson functions. The Re–Re bond distance is the same, 2.625(1) Å, for both compounds, and falls within the range of M–M bond distance established for similar Re–Re double bonds. Here again, the chirality of the *meso*-tetraphos-1 ligand drives these compounds to adopt a geometrical isomer type of 1,2,7,8 (4), which has been first found in 1,2,7,8-Mo_2Cl_6(*meso*-eLTTP) (**2**) discussed earlier. It is interesting to notice that although the *meso*-eLTTP and *meso*-tetraphos-1 ligands have different chain lengths for the central connecting chains between P atoms, and also different terminal -PR_2 groups, they adopt the same geometry. This may answer our earlier question concerning whether the changes in the connecting chain lengths between the P atoms and/or in the terminal groups might play an important role in changing the geometry of this type of compound. It seems clear now that the chirality of the meso or racemic diastereomer is a crucial factor in determining the geometry of the ESBO compounds with the tetraphosphine ligands.

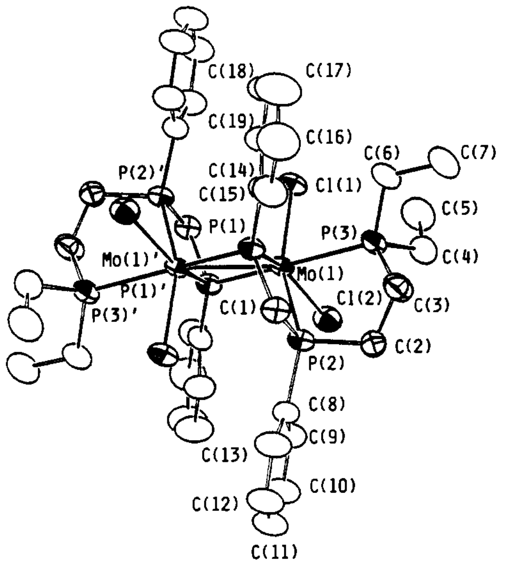

Figure 4. ORTEP drawing of *meso*-$Mo_2Cl_4[Et_2P(CH_2)_2P(Ph)CH_2P(Ph)_2]_2 \cdot 2C_6H_6$ (**4**). Thermal ellipsoids are drawn at the 50% probability level.

Table VIII. Selected Bond Lengths (Å) and Angles (deg) for *meso*-$Mo_2Cl_4[Et_2P(CH_2)_2P(Ph)CH_2P(Ph) \cdot 2C_6H_6$ (4)[a]

	Distances		
Mo(1)–Mo(1)′	2.8312(3)	Mo(1)–P(3)	2.5727(8)
Mo(1)–Cl(1)	2.425(1)	Mo(1)–Cl(2)	2.472(1)
Mo(1)–P(1)	2.3945(9)	Mo(1)′–P(1)	2.3861(8)
Mo(1)–P(2)	2.499(1)		
	Angles		
Mo(1)–Mo(1)′–Cl(1)	105.45(2)	Cl(2)–Mo(1)–P(3)	83.37(3)
Mo(1)–Mo(1)′–Cl(2)	132.32(2)	P(1)–Mo(2)–P(1)′	107.37(3)
Mo(1)–Mo(1)′–P(1)	53.55(2)	P(1)–Mo(1)–P(2)	65.91(3)
Mo(1)′–Mo(1)–P(1)	53.82(2)	P(1)–Mo(1)–P(3)	87.82(3)
Mo(1)–Mo(1)′–P(2)	88.53(2)	P(1)′–Mo(1)–P(2)	112.28(3)
Mo(1)–Mo(1)′–P(3)	141.09(3)	P(1)′–Mo(1)–P(3)	164.02(3)
Cl(1)–Mo(1)–Cl(2)	97.81(3)	P(2)–Mo(1)–P(3)	78.05(3)
Cl(1)–Mo(1)–P(1)	107.20(3)	Mo(1)–P(1)–Mo(1)′	72.63(2)
Cl(1)–Mo(1)′–P(1)	91.10(3)	Mo(1)–P(1)–C(1)	102.1(1)
Cl(1)–Mo(1)–P(2)	156.60(3)	Mo(1)′–P(1)–C(1)	112.48(9)
Cl(1)–Mo(1)–P(3)	79.37(3)	Mo(1)–P(2)–C(1)	99.1(1)
Cl(2)–Mo(1)–P(1)	151.44(4)	Mo(1)–P(2)–C(2)	109.3(1)
Cl(2)–Mo(1)′–P(1)	85.27(3)	Mo(1)–P(3)–C(3)	110.9(1)
Cl(2)–Mo(1)–P(2)	85.66(3)		

[a] Numbers in parentheses are estimated standard deviations in the least significant digit.

Experimental Procedures

General Data. All manipulations were carried out under an atmosphere of argon unless otherwise specified. Standard Schlenk and vacuum line techniques were used. Commercial grade solvents were dried and deoxygenated by refluxing at least 24 h over the appropriate reagents and freshly distilled before use. Toluene, THF, benzene, diethyl ether, and hexanes were purified by distillation from potassium/sodium benzophenone ketyl, and acetonitrile was purified from CaH_2.

The tetraphos-1 ligand, which is a mixture of the meso and racemic diastereomers, was purchased from Strem Chemicals and used as received. The *meso*-eLTTP ligand and the 1:1 mixture of the meso and racemic diastereomers were synthesized according to the published procedure.[9b] $Mo_2Cl_4(PEt_3)_4$,[13,14] $Mo_2(O_2CCF_3)_4$,[15] and $(NBu^n_4)_2Re_2Cl_8$[16] were also prepared according to the published procedures. The UV/vis data were collected on a Cary 17-D spectrophotometer. Analyses were done by Galbraith Laboratories, Inc. The $^{31}P\{^1H\}$ NMR spectra were recorded in a CD_2Cl_2/CH_2Cl_2 solvent mixture on a Varian XL-200 spectrometer. The $^{31}P\{^1H\}$ NMR chemical shift values were referenced externally and are reported relative to 85% H_3PO_4.

Table IX. Selected Bond Lengths (Å) and Angles (deg) for 1,2,7,8-Re_2Cl_6(*meso*-tetraphos-1) (5)[a]

	Distances		
Re(1)–Re(2)	2.625(1)	Re(2)–Cl(1)	2.372(5)
Re(1)–Cl(1)	2.356(5)	Re(2)–Cl(2)	2.401(5)
Re(1)–Cl(2)	2.414(5)	Re(2)–Cl(5)	2.399(5)
Re(1)–Cl(3)	2.413(5)	Re(2)–Cl(6)	2.397(5)
Re(1)–Cl(4)	2.389(5)	Re(2)–P(3)	2.425(6)
Re(1)–P(1)	2.497(5)	Re(2)–P(4)	2.469(6)
Re(1)–P(2)	2.382(6)		
	Angles		
Re(2)–Re(1)–Cl(1)	56.6(1)	Re(1)–Re(2)–Cl(2)	57.2(1)
Re(2)–Re(1)–Cl(2)	56.7(1)	Re(1)–Re(2)–Cl(5)	96.6(1)
Re(2)–Re(1)–Cl(3)	99.4(1)	Re(1)–Re(2)–Cl(6)	142.6(1)
Re(2)–Re(1)–Cl(4)	140.0(1)	Re(1)–Re(2)–P(3)	103.2(1)
Re(2)–Re(1)–P(1)	135.7(1)	Re(1)–Re(2)–P(4)	134.3(1)
Re(2)–Re(1)–P(2)	98.0(1)	Cl(1)–Re(2)–Cl(2)	112.5(2)
Cl(1)–Re(1)–Cl(2)	112.6(2)	Cl(1)–Re(2)–Cl(5)	90.5(2)
Cl(1)–Re(1)–Cl(3)	94.7(2)	Cl(1)–Re(2)–Cl(6)	161.2(2)
Cl(1)–Re(1)–Cl(4)	163.1(2)	Cl(1)–Re(2)–P(3)	102.8(2)
Cl(1)–Re(1)–P(1)	79.2(2)	Cl(1)–Re(2)–P(4)	78.4(2)
Cl(1)–Re(1)–P(2)	94.4(2)	Cl(2)–Re(2)–Cl(5)	88.6(2)
Cl(2)–Re(1)–Cl(3)	87.5(2)	Cl(2)–Re(2)–Cl(6)	85.6(2)
Cl(2)–Re(1)–Cl(4)	84.3(2)	Cl(2)–Re(2)–P(3)	99.8(2)
Cl(2)–Re(1)–P(1)	166.6(2)	Cl(2)–Re(2)–P(4)	167.9(2)
Cl(2)–Re(1)–P(2)	102.7(2)	Cl(5)–Re(2)–Cl(6)	84.7(2)
Cl(3)–Re(1)–Cl(4)	86.0(2)	Cl(5)–Re(2)–P(3)	159.9(2)
Cl(3)–Re(1)–P(1)	85.2(2)	Cl(5)–Re(2)–P(4)	86.0(2)
Cl(3)–Re(1)–P(2)	162.6(2)	Cl(6)–Re(2)–P(3)	77.9(2)
Cl(4)–Re(1)–P(1)	84.1(2)	Cl(6)–Re(2)–P(4)	83.1(2)
Cl(4)–Re(1)–P(2)	81.0(2)	P(3)–Re(2)–P(4)	82.1(2)
P(1)–Re(1)–P(2)	81.9(2)	Re(1)–Cl(1)–Re(2)	67.5(1)
Re(1)–Re(2)–Cl(1)	56.0(1)	Re(1)–Cl(2)–Re(2)	66.1(1)

[a] Numbers in parentheses are estimated standard deviations in the least significant digit.

Table X. Selected Bond Lengths (Å) and Angles (deg) for 1,2,7,8-Re_2Cl_6(*meso*-tetraphos-1)·$(CH_3CH_2)_2O$ (6)[a]

	Distances		
Re(1)–Re(2)	2.625(1)	Re(2)–P(3)	2.398(8)
Re(1)–Cl(1)	2.348(7)	Re(2)–P(4)	2.469(8)
Re(1)–Cl(2)	2.409(7)	Re(2)–Cl(1)	2.368(7)
Re(1)–Cl(3)	2.403(7)	Re(2)–Cl(2)	2.419(7)
Re(1)–Cl(4)	2.399(8)	Re(2)–Cl(5)	2.409(8)
Re(1)–P(1)	2.496(8)	Re(2)–Cl(6)	2.412(8)
Re(1)–P(2)	2.377(8)		
	Angles		
Re(2)–Re(1)–Cl(1)	56.5(2)	Re(1)–Re(2)–Cl(6)	98.0(2)
Re(2)–Re(1)–Cl(2)	57.2(2)	Re(1)–Re(2)–P(3)	102.2(2)
Re(2)–Re(1)–Cl(3)	140.8(2)	Re(1)–Re(2)–P(4)	135.8(2)
Re(2)–Re(1)–Cl(4)	97.2(2)	Cl(1)–Re(2)–Cl(2)	112.2(2)
Re(2)–Re(1)–P(1)	136.7(2)	Cl(1)–Re(2)–Cl(5)	163.3(3)
Re(2)–Re(1)–P(2)	97.6(2)	Cl(1)–Re(2)–Cl(6)	92.8(3)
Cl(1)–Re(1)–Cl(2)	113.2(2)	Cl(1)–Re(2)–P(3)	98.9(3)
Cl(1)–Re(1)–Cl(3)	162.6(3)	Cl(1)–Re(2)–P(4)	80.0(3)
Cl(1)–Re(1)–Cl(4)	92.6(2)	Cl(2)–Re(2)–Cl(5)	84.3(2)
Cl(1)–Re(1)–P(1)	80.2(3)	Cl(2)–Re(2)–Cl(6)	88.6(2)
Cl(1)–Re(1)–P(2)	94.1(3)	Cl(2)–Re(2)–P(3)	101.9(3)
Cl(2)–Re(1)–Cl(3)	84.2(2)	Cl(2)–Re(2)–P(4)	166.1(2)
Cl(2)–Re(1)–Cl(4)	87.8(2)	Cl(5)–Re(2)–Cl(6)	84.6(3)
Cl(2)–Re(1)–P(1)	165.6(2)	Cl(5)–Re(2)–P(3)	79.5(3)
Cl(2)–Re(1)–P(2)	101.7(3)	Cl(5)–Re(2)–P(4)	83.3(3)
Cl(3)–Re(1)–Cl(4)	87.4(3)	Cl(6)–Re(2)–P(3)	159.9(3)
Cl(3)–Re(1)–P(1)	82.4(3)	Cl(6)–Re(2)–P(4)	84.0(3)
Cl(3)–Re(1)–P(2)	82.2(3)	P(3)–Re(2)–P(4)	82.0(3)
Cl(4)–Re(1)–P(1)	86.4(3)	Re(1)–Cl(1)–Re(2)	67.7(2)
Cl(4)–Re(1)–P(2)	165.1(3)	Re(1)–Cl(2)–Re(2)	65.9(2)
P(1)–Re(1)–P(2)	81.7(3)	Re(1)–Re(2)–Cl(2)	56.9(2)
Re(1)–Re(2)–Cl(1)	55.8(2)	Re(1)–Re(2)–Cl(5)	140.9(2)

[a] Numbers in parentheses are estimated standard deviations in the least significant digit.

Preparation of $Mo\overset{4}{-}MoCl_4$(*meso*-eLTTP) (1) and 1,2,7,8-Mo_2Cl_6(*meso*-eLTTP)·C_6H_6 (2). In a 50-mL flask, $Mo_2(O_2CCF_3)_4$ (0.30 g, 0.47 mmol) and *meso*-eLTTP (0.30 g, 0.65 mmol) were dissolved in 15

---

(13) Cotton, F. A.; Daniels, L. M.; Powell, G. L.; Kahaian, A. J.; Smith, T. J.; Vogel, E. F. *Inorg. Chim. Acta* **1988**, *144*, 109.

(14) Glicksman, H. D.; Hamer, A. D.; Smith, T. J.; Walton, R. A. *Inorg. Chem.* **1976**, *15*, 2205.

(15) Cotton, F. A.; Norman, J. G. *J. Coord. Chem.* **1971**, *1*, 161.

(16) Barder, T. J.; Walton, R. A. *Inorg. Synth.* **1985**, *23*, 116.

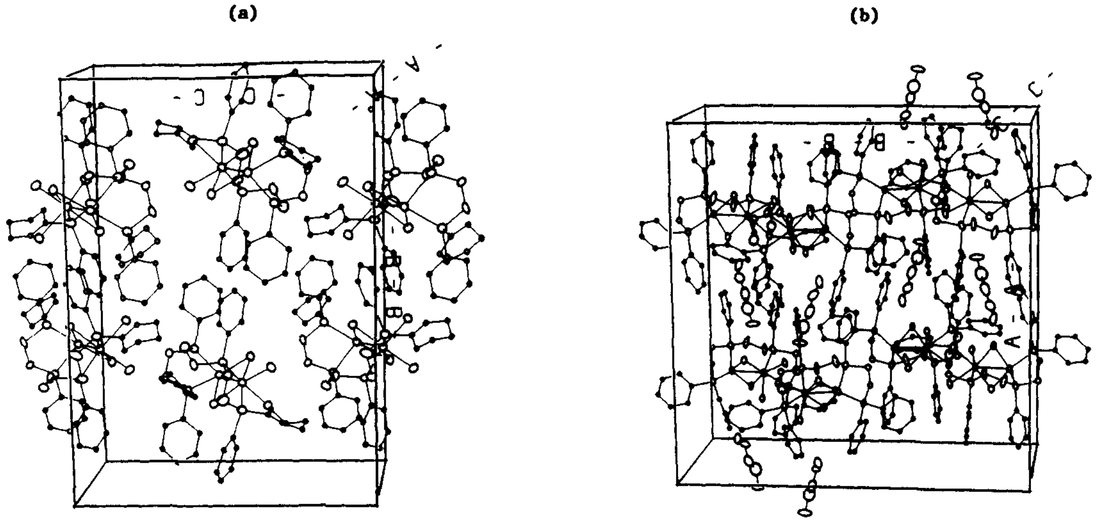

Figure 5. (a) Stereoview of the unit cell packing in compound **5**. (b) Stereoview of the unit cell packing in compound **6**.

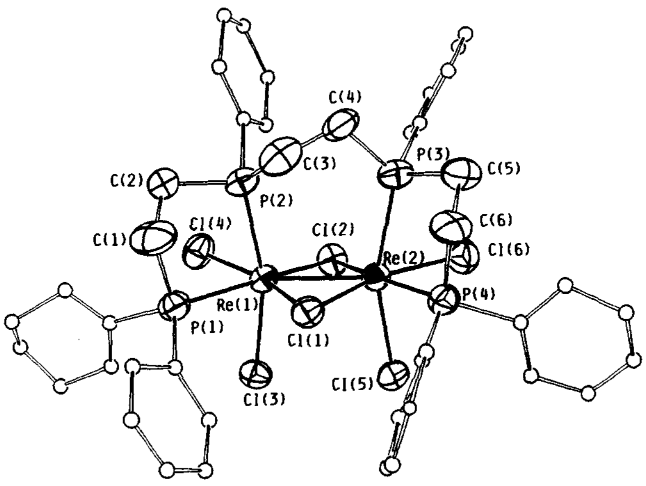

Figure 6. ORTEP drawing of 1,2,7,8-Re$_2$Cl$_6$(*meso*-tetraphos-1) (**5**). Thermal ellipsoids are drawn at the 50% probability level. For clarity, all of the carbon atoms except those on the ethylene connecting chains between phosphorus atoms assume an arbitrary thermal ellipsoid.

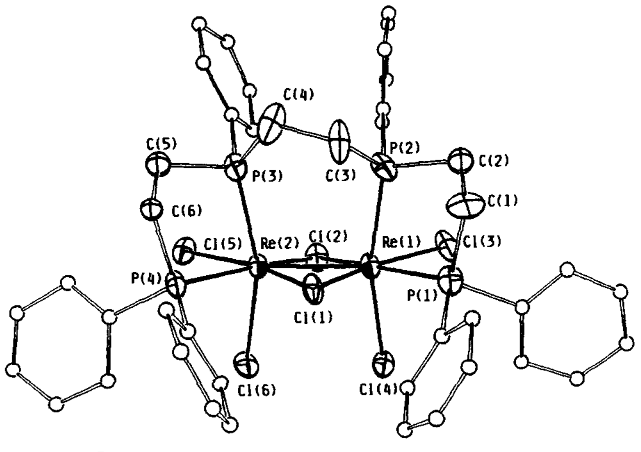

Figure 7. ORTEP drawing of 1,2,7,8-Re$_2$Cl$_6$(*meso*-tetraphos-1)·(CH$_3$CH$_2$)$_2$O (**6**). Thermal ellipsoids are drawn at the 50% probability level. For clarity, all of the carbon atoms except those on the ethylene connecting chains between phosphorus atoms assume an arbitrary thermal ellipsoid.

mL of THF, and then Me$_3$SiCl (0.4 mL, 3.2 mmol) was added. The reaction mixture first turned to blue-green, and then a blue precipitate **1** soon began to form, while the solution remained green. After 24 h, the blue precipitate was filtered out, washed with hexanes, and dried under the reduced pressure. Yield: 65–75%. Anal. Calc for Mo$_2$Cl$_4$P$_4$C$_{25}$H$_{40}$: C, 37.81; H, 4.58. Found for **1**: C, 37.27; H, 5.12. UV/vis of **1**: 625, 487, 315 nm. ^{31}P{^{1}H} NMR of **1**: 45.67 (doublet), 55.68 ppm (doublet), J_{P-P} = 4 Hz.

The blue precipitate **1** was dissolved in CH$_2$Cl$_2$ to give a blue solution. At room temperature, it changed to a red solution over a period of 12 h. This red solution was then layered with 20 mL of a benzene/hexane (volume ratio 1:3) mixture. Small red crystals of **2** grew in 2 weeks in 10–15% yield. UV/vis of **2**: 392 nm.

Preparation of Mo$_2$Cl$_4$(eLTTP) (3) and *meso*-Mo$_2$Cl$_4$[Et$_2$P(CH$_2$)$_2$P(Ph)CH$_2$P(Ph)]$_2$·2C$_6$H$_6$ (4). Mo$\overset{4}{-}$MoCl$_4$(PEt$_3$)$_4$ (0.20 g, 0.25 mmol) and the mixture of the meso and racemic diastereomers of eLTTP ligand (1.8 mL of 0.15 M toluene solution, 0.27 mmol) were placed in a three-neck flask equipped with a reflux condenser. Toluene (20 mL) was then added. This mixture was refluxed for 21 h to yield a brown solution and a green solid (**3**). The solid was filtered out, washed with hexanes, and then dried in vacuum. Yield: 55–65%. Anal. Calc for Mo$_2$Cl$_4$P$_4$C$_{25}$H$_{40}$: C, 37.81; H, 4.58. Found for **3**: C, 37.82; H, 5.12. UV/vis of **3**: 705, 418, 375 nm. ^{31}P{^{1}H} NMR of **3**: 48.29 (doublet), 55.79 ppm (doublet), J_{P-P} = 3 Hz.

This green solid was dissolved in CH$_2$Cl$_2$ to give a brown-green solution, which was then layered with the benzene/THF (1:1.5) mixture. Several brown prismatic crystals of **4** and some dark green crystals (ca. 5% yield) formed several weeks later, and the solution changed to brown. Although we have collected data on one of the dark green crystals, no proper model was found to solve the structure.

Preparation of 1,2,7,8-Re$_2$Cl$_6$(*meso*-tetraphos-1) (5), 1,2,7,8-Re$_2$Cl$_6$(*meso*-tetraphos-1)·(CH$_3$CH$_2$)$_2$O (6), and Re$_2$Cl$_4$(tetraphos-1) (7). (NBu$^n{}_4$)$_2$Re$_2$Cl$_8$ (0.30 g, 0.26 mmol) and the mixture of meso and racemic diastereomers of tetraphos-1 ligand (0.21 g, 0.31 mmol) were suspended in 20 mL of CH$_2$Cl$_2$ in a three-neck flask equipped with a reflux condenser. This suspension was stirred and heated at reflux temperature for 26 h to yield a brown-yellow solution and a red solid. This red solid was filtered out, washed with hexanes, and then dried in vacuum. Yield of this red solid: 5–15%. UV/vis: 480, 382 nm.

Two different types of red crystals, thin plates and needles, were obtained from slow diffusion of a hexane/diethyl ether (1:2) mixture into the MeCN solution of the red solid. They have been structurally determined to be compounds **5** and **6**.

The volume of the brown-yellow mother liquor was reduced to ca. 10 mL using vacuum evaporation. A 50-mL volume of hexanes was then added to give a brown-yellow precipitate, which was filtered out, washed with hexanes and diethyl ether, and dried overnight under reduced pressure to give a brown-yellow product **7**. Yield: 65–75%. Anal. Calc for Re$_2$Cl$_4$P$_4$C$_{42}$H$_{42}$: C, 42.54; H, 3.58; Cl, 11.98. Found for **7**: C, 45.65; H, 4.45; Cl, 13.55. UV–vis: 682, 432 nm. ^{31}P{^{1}H} NMR of **7** at 273 K: four multiplets at 53.6, 51.1, 41.5, and 32.1 ppm.

X-Ray Crystallography

The structures of compounds **2** and **4**–**6** were determined by a general procedure that has been fully described elsewhere.[17] Data reduction was carried out by standard methods with the use of well-established

---

(17) (a) Bino, A.; Cotton, F. A.; Fanwick, P. E. *Inorg. Chem.* **1979**, *18*, 3558. (b) Cotton, F. A.; Frenz, B. A.; Deganello, G.; Shaver, A. *J. Organomet. Chem.* **1979**, *50*, 227.

computational procedures.[18] The computations were done with Enraf-Nonius SDP and SHELX-76 software on a VAX computer. The structure factors were obtained after Lorentz and polarization corrections. Empirical absorption corrections based on azimuthal (ψ) scans of reflections of Eulerian angle χ near 90° were applied to all the data.[19] Pertinent crystallographic information on all structures is given in Table II. Tables III–VI list the positional and thermal parameters for complexes **2** and **4–6**, respectively. Tables VII–X list selected bond distances and angles for each of the structures.

Compound 2. A brown-red crystal with dimensions 0.03 × 0.08 × 0.10 mm was mounted on the tip of a quartz fiber with epoxy cement. The unit cell constants and axial photographs were consistent with a triclinic lattice, and the space group $P\bar{1}$ was chosen and proved to be correct by the successful refinement. The diffusion data were collected on a Rigaku AFC5R with Cu Kα radiation. No obvious decay was found during the data collection.

The direct methods program in SHELXS-86 led to the location of the positions of the molybdenum atoms and their coordinated atoms. The remaining non-hydrogen atoms, including the benzene molecule, were found from a series of alternating difference Fourier maps and least-squares refinements. All the non-hydrogen atoms were refined anisotropically to convergence in the final refinement.

Compound 4. A brown block-shaped crystal with dimensions 0.30 × 0.30 × 0.25 mm was coated with a thin layer of epoxy cement and mounted on the tip of a quartz fiber. The unit cell constants were determined from 25 reflections with 2θ values in the range from 48.3 to 58.6°. These were consistent with a triclinic crystal system, and the space group $P\bar{1}$ was chosen and proved to be correct by the successful refinement. The diffraction data were collected on a Rigaku AFC5R with Cu Kα radiation. Routine ω–2θ data collection was used. Three check reflections monitored throughout the data collection displayed no significant decay in intensity or change in the crystal orientation.

The direct methods program in SHELXS-86 led to the location of positions of one independent Mo atom of the dinuclear skeleton and its coordinated atoms. The remaining non-hydrogen atoms, including the benzene molecule, were found in a series of alternating difference Fourier maps and least-squares refinements. All the non-hydrogen atoms were refined anisotropically to convergence. The hydrogen atoms were then placed in the calculated positions, and their thermal parameters were constrained to the calculated values, which were, correspondingly, three times the values of the thermal parameters of the carbon atoms to which these hydrogen atoms are bonded. The positions of these hydrogen atoms were then refined isotropically to convergence.

Compound 5. A brown-red, thin plate crystal with dimensions 0.20 × 0.15 × 0.04 mm was coated with a thin layer of epoxy cement and mounted on the tip of a quartz fiber. The unit cell constants were determined from 25 reflections with 2θ values in the range from 28.4 to 57.9°. These were consistent with a monoclinic crystal system, and the space group $P2_1/c$ was determined from the systematic absences. The diffraction data were collected on a Rigaku AFC5R with Cu Kα radiation. Routine ω–2θ data collection was used.

A three-dimensional Patterson synthesis led to the location of the positions of the rhenium atoms and their coordinated atoms. The subsequent alternating difference Fourier maps and the least-squares refinements gave the positions of all the remaining non-hydrogen atoms. The program DIFABS was used to correct for absorption after all the non-hydrogen atoms had been located and isotropically refined. All the non-hydrogen atoms were then refined anisotropically, leading to the final residuals as $R = 0.0486$ and $R_w = 0.0657$ after convergence. No solvent molecule was found. The final difference electron density map had no significant features other than some "ghost" peaks very close to the Re(1) and Re(2) atoms.

Compound 6. A brown-red needle crystal with the dimensions 0.30 × 0.25 × 0.10 mm was mounted on the tip of a quartz fiber with epoxy resin. The unit cell constants were determined from 25 reflections with 2θ values in the range from 20.3 to 28.0°. The unit cell constants and the axial photographs were consistent with an orthorhombic crystal system, and the space group *Pbca* was determined from the systematic absences. The diffraction data were collected on a Syntex P3 diffractometer with Mo Kα radiation. Routine ω–2θ data collection was used.

A three-dimensional Patterson synthesis provided the positions of the rhenium atoms and their coordinated atoms. The remaining non-hydrogen atoms were found in a series of alternating difference Fourier maps and least-squares refinements. These atoms were refined anisotropically. Some of the atoms with nonpositive definite thermal parameters were then refined isotropically to convergence. A difference Fourier map then revealed a chain of five peaks, which were first refined isotropically as C atoms. The middle atom was then changed to O(1), and all atoms in this solvent molecule were refined anisotropically to convergence, with $R = 0.062\,17$ and $R_w = 0.075\,06$. The final difference electron density map had no significant features other than some "ghost" peaks very close to the Re(1) and Re(2) atoms.

Acknowledgment. Financial support from the National Science Foundation is appreciated.

Supplementary Material Available: Full lists of crystallographic data, bond distances, bond angles, positional and thermal parameters for the H atoms of **4**, and anisotropic thermal parameters (32 pages). Ordering information is given on any current masthead page.

---

[18] Crystallographic computing was done on a local area VAX cluster employing the VAX/VMS V5.4 computer.

[19] North, A. C. T.; Phillips, D. C.; Mathews, F. S. *Acta Crystallogr., Sect. A* **1968**, *24*, 351.

[20] Cotton, F. A.; Mandal, S. K. *Inorg. Chem.* **1992**, *32*, 1267.

[21] Canich, J. M.; Cotton, F. A.; Daniels, L. M.; Lewis, D. B. *Inorg. Chem.* **1987**, *26*, 4046.

[22] Chakravorty, A. R.; Cotton, F. A.; Diebold, M. P.; Lewis, D. B.; Roth, W. J. *J. Am. Chem. Soc.* **1986**, *108*, 971.

[23] Cotton, F. A.; Daniels, L. M.; Dunbar, K. R.; Falvello, L. R.; O'Connor, C. J.; Price, A. C. *Inorg. Chem.* **1991**, *30*, 2509.

[24] Cotton, F. A.; Eglin, J. L.; James, C. A.; Luck, R. L. *Inorg. Chem.* **1992**, *31*, 5308.

[25] Cotton, F. A.; James, C. A.; Luck, R. L. *Inorg. Chem.* **1991**, *30*, 4370.

[26] Jaecker, J. A.; Robinson, W. R.; Walton, R. A. *J. Chem. Soc., Dalton Trans.* **1975**, 698.

[27] Agaskar, P. A.; Cotton, F. A.; Dunbar, K. R.; Falvello, L. R.; O'Connor, C. J. *Inorg. Chem.* **1987**, *26*, 4051.

[28] Cotton, F. A.; Dunbar, K. R. *Inorg. Chem.* **1987**, *26*, 1305.